Computers and Mathematics with Applications 59 (2010) 3687–3699

Contents lists available at ScienceDirect

Computers and Mathematics with Applications

journal homepage: www.elsevier.com/locate/camwa

On the choice of stabilizing sub-grid for convection–diffusion problem on rectangular grids

A.I. Neslitürk *

Izmir Institute of Technology, Department of Mathematics, 35430, Izmir, Turkey

ARTICLE INFO

Article history:
Received 12 November 2009
Received in revised form 25 March 2010
Accepted 5 April 2010

Keywords:
Stabilized FEM
Convection–diffusion problem
Stabilizing sub-grid

ABSTRACT

A stabilizing sub-grid which consists of a single additional node in each rectangular element is analyzed for solving the convection–diffusion problem, especially in the case of small diffusion. We provide a simple recipe for spotting the location of the additional node that contributes a very good stabilizing effect to the overall numerical method. We further study convergence properties of the method under consideration and prove that the standard Galerkin finite element solution on augmented grid produces a discrete solution that satisfies the same type of a priori error estimates that are typically obtained with the SUPG method. Some numerical experiments that confirm the theoretical findings are also presented.

1. Introduction

It is well known that the exact solution of the convection–diffusion problem may exhibit very narrow regions where the solution and its derivatives change sharply. If the standard Galerkin Finite Element Method (FEM) with a discretization scale which is too big to resolve the layers is employed, the numerical method will produce oscillations that pollute the whole domain. To properly resolve the layers, the mesh size must be of the same size as the ratio between diffusion and convection. However, this choice would make the classical FEM impractical for real-world problems.

Several approaches proposed to cure this problem can be found in the literature. One of the most popular approaches, where the finite dimensional function space in the finite element formulation is enriched with a certain type of bubble functions in order to gain control on the derivatives of the FEM solution, is known as the Residual-free bubble (RFB) method [1]. The RFB method has been used with success to stabilize a certain number of problems, including the convection-dominated flows [2,3]. The advantage of this approach is not only its generality, but also the fact that its error analysis can be performed in many cases of interest [4–6]. Further, the RFB method contributes an additional term to the standard Galerkin formulation, which has a structure identical to the mesh-dependent term in the SUPG method in the case of piecewise linears on a triangular discretization [7,1]. This equivalence can be extended to the case of bilinear interpolations on a rectangular discretization if the flow is not aligned with the diagonals of the element [8].

However, the implementation of the RFB method requires the solution of a local boundary value problem with a vanishing boundary condition, which is not easier to solve than the original problem except that the problem is posed over an element domain which is either a triangle or a quadrangle. Sometimes taking the shape of element domain into consideration, it is desirable to devise a numerical algorithm to obtain a cheap approximate solution to the local problem. To this end, several researchers dealt with finding an approximate solution having some level of precision to the local problem with the use of a suitable sub-grid consisting of a few nodes [9–12]. The resulting numerical methods were implemented with success and they produced approximations consistent with the physical configuration of the problem but they were lacking of a

* Tel.: +90 232 750 7522; fax: +90 232 750 7509.
E-mail address: alinesliturk@iyte.edu.tr.

0898-1221/$ – see front matter © 2010 Elsevier Ltd. All rights reserved.
doi:10.1016/j.camwa.2010.04.002

rigorous error analysis similar to the ones that we have for the SUPG or the RFB method. More recently, some conditions on the choice of sub-grid that guarantees the corresponding numerical method satisfies the same type a priori error estimates as we have for the SUPG method were introduced in [13]. In a couple of subsequent papers, several stabilizing sub-grids which consist of a single additional node in each triangular element were proposed and it is proved that the corresponding numerical methods satisfy the same a priori error estimates as the SUPG and the exact RFB method [14,15].

In this work, we consider a decomposition of the domain into rectangles where the sides are parallel to the coordinate axes. Regarding this special case of decomposition, we propose and analyze a method based on augmenting a given coarse mesh by adding a suitably located single internal node inside each rectangle and forming a sub-grid by joining the additional point to a coarse grid points. We then solve the problem on the augmented grid in the framework of the Standard Galerkin FEM. We further prove that the method under consideration satisfies the same a priori error estimates as the one for the SUPG method by proving that the numerical method with the present choice of sub-grid satisfies the conditions stated in [13].

The layout of the paper is as follows. In Section 2 we briefly recall the basic ideas of the RFB method and describe the related numerical method on the augmented grid. In Section 3 we display how to choose the single internal node in an arbitrary rectangular element and determine its precise location. The corresponding a priori error estimates for the formulation is proved in Section 4. Finally, we present several numerical experiments to validate the method in Section 5.

2. The RFB method

Consider the following linear elliptic convection–diffusion problem in a bounded polygonal domain Ω in $\mathbb{R}^2$:

$$\begin{cases} Lu = f & \text{in } \Omega, \\ u = 0 & \text{on } \partial\Omega, \end{cases} \tag{1}$$

where

$$Lu = -\epsilon\triangle u + \beta \cdot \nabla u.$$

We assume that the diffusion coefficient ϵ is a positive constant. Let us recall the classical variational formulation of the problem (1): Find $u \in H_0^1(\Omega)$ such that

$$a(u, v) = (f, v) \quad \text{for all } v \in H_0^1(\Omega) \tag{2}$$

where

$$a(u, v) = \epsilon \int_\Omega \nabla u \cdot \nabla v \mathrm{d}\Omega + \int_\Omega (\beta \cdot \nabla u) v \mathrm{d}\Omega$$

is a continuous and coercive bilinear form on the Hilbert space $H_0^1(\Omega)$, and (f, v) denotes the scalar product of f and v in $L^2(\Omega)$.

Let τ_h be a decomposition of Ω and let V_P be a finite dimensional subspace of $H_0^1(\Omega)$ whose elements are polynomial of a certain degree on each $K \in \tau_h$. We further assume that the convection field β and the right-hand side f are piecewise constants with respect to the decomposition τ_h. It is well known that the standard finite element method becomes unstable when the value of ϵ is small compared to $|\beta|h$ and various possible approaches to stabilize the numerical algorithm exist in the literature. The residual-free bubble (RFB) method, whose basic idea consists of enriching the finite dimensional space V_P by the RFB functions, is among the most popular ones and has been receiving considerable attention. Since the bubble functions vanishes on element boundary, they can be eliminated locally, yielding a formulation in the original discrete space with modified operators. To give some more detail of the method, let us consider the Galerkin approximation of the problem (1) in the following space:

$$V_h = V_P \oplus V_B = V_P \bigoplus_{K \in \tau_h} B^K$$

where B^K, specified below in (6), is a finite dimensional subspace of $H_0^1(K)$. Thus, for any $v_h \in V_h$ we can split it into a polynomial part $v_P \in V_P$ and into a bubble part $v_B \in V_B$ in a unique way. Then the variational problem (2) is approximated as follows: Denoting the restriction of the bubble component u_B of u_h in a typical element K by $u_{B,K}$, find $u_h = u_P + u_B \in V_P \bigoplus V_B$ for all $v_P \in V_P$ and $v_{B,K} \in B^K$, such that,

$$a(u_P + u_B, v_P) = (f, v_P) \tag{3}$$

$$a(u_P + u_{B,K}, v_{B,K})_K = (f, v_{B,K})_K \tag{4}$$

where $(.,.)_K$ indicates the integrals involved are restricted to the element K. Let us introduce an operator $M_K : L_2(K) \to H_0^1(K) \bigcap H^2(K)$ such that it takes every right-hand side function g to the unique solution φ of

$$L\varphi = g \quad \text{in } K \quad \text{with } \varphi = 0 \quad \text{on } \partial K. \tag{5}$$

Observe that the Eq. (4) determines $u_{B,K}$ in terms of f and u_P through the relation

$$u_{B,K} = M_K(f - L u_P). \tag{6}$$

Introducing the formal adjoint L^* of L on K with the property that $a(v_B, v_P)_K = (v_B, L^* v_P)_K$ holds for all $v_B \in V_B$ and $V_P \in V_P$ and substituting (6) into the Eq. (3), we get a representation for the effect of the residual-free bubbles onto the polynomial

component of the approximation:

$$a(u_P, v_P) + \sum_{K\in\tau_h} (M_K(f - Lu_P), L^* v_P)_K = (f, v_P) \quad \forall v_P \in V_P. \tag{7}$$

If τ_h is a decomposition of Ω into triangles and V_P is a finite dimensional subspace of $H_0^1(\Omega)$ whose elements are linear functions on each $K \in \tau_h$, then it can be shown that the effect of the bubbles, which is identified with an additional term in (7), has an identical structure with the mesh-dependent term in the SUPG method [3]. Further, a priori error estimates of the RFB method for triangular elements can be proved (see [4]).

Now let us assume τ_h be a decomposition of Ω into rectangles with the sides parallel to the coordinate axes and V_P be a finite dimensional subspace of $H_0^1(\Omega)$ whose elements are bilinear functions on each $K \in \tau_h$. It can be shown that the additional term in (7) through the effect of the bubbles is responsible for the stability of the corresponding numerical method and it is equivalent to the mesh-dependent term in the SUPG method in both convection-dominated and diffusion-dominated cases except when the direction of the flow is aligned with the diagonal of the elements [8]: There exist constants μ_i, $(i = 1, 2)$ of order $O(h)$ in convection-dominated case and $O(h^2)$ in diffusion-dominated case, respectively, such that

$$\sum_{K\in\tau_h} \mu_1 \|\beta \cdot \nabla v_P\|^2 \le S_{RFB}(v_P, v_P) \le \sum_{K\in\tau_h} \mu_2 \|\beta \cdot \nabla v_P\|^2 \quad \forall v_P \in V_P \tag{8}$$

where

$$S_{RFB}(u_P, v_P) = \sum_{K\in\tau_h} \left(M_K(-Lu_P), L^* v_P\right)_K.$$

Thus the resulting numerical scheme is nothing more than a method of streamline diffusion type and the typical a priori error estimates can be obtained for bilinear elements (see [5]).

However, computer implementation of the stabilizing term S_{RFB} requires the exact solution of a number of boundary value problems describing the bubble functions inside each element which may be difficult to solve as much as the original problem. Therefore it is important to obtain a cheap approximate solution to the local bubble problem so that the corresponding numerical approximation over the original discretization satisfies the same a priori error estimates as the SUPG method. In the case of triangular elements, several numerical methods were proposed to provide an approximate solution to local bubble problem with the use of a suitable sub-grid [14,9,10,3]. The common point of these attempts was to construct a low dimensional sub-grid space B_h^K in such a way that the solution of the discrete local problem could produce an approximation b_h^K to b^K such that

$$\int_K b_h^K \simeq \int_K b^K.$$

From a different point of view, these methods can be regarded as a standard Galerkin method on an augmented grid (the original grid plus the sub-grid) for which the finite element space V_h^A is a finite dimensional subspace of V_h. It can be proved that if the sub-grid space is chosen to be $B_h^K = V_h^A \bigcap B^K$ and it satisfies certain sufficient conditions then the solution of the problem

$$\begin{cases} \text{Find} \quad u_h^A \in V_h^A \quad \text{such that} \\ a(u_h^A, v_h^A) = (f, v_h^A) \quad \forall\, v_h^A \in V_h^A \end{cases} \tag{9}$$

satisfies the same type a priori error bounds as the SUPG method [13]. Explicit examples of sub-grids with this property were presented and analyzed in [14,15] for triangular discretizations.

In the following section, we are going to display how to choose a suitable sub-grid consisting of a single additional node per element in a rectangular discretization. Then we show that the present choice of the sub-grid satisfies the sufficient conditions in [13] and thus, a priori error estimate similar to the one in the SUPG method hold true for the corresponding numerical method (9).

3. The choice of the sub-grid

Let us assume τ_h be a decomposition of Ω into rectangles with the sides parallel to the coordinate axes and K be any rectangle in τ_h with side of lengths l_1 and l_2. We assume the standard shape regularity condition, for each $K \in \tau_h$, that there is a positive constant C_1 such that

$$C_1 h_K \le \min(l_1, l_2) \le \max(l_1, l_2) \le h_K \tag{10}$$

where h_K is the diameter of the element K and measured by the length of the diagonal. Since all computations are carried out in a fixed element, we mostly drop subindex K and use h instead of h_K. We further assume that, without loss of generality, the components of the convection field $\overrightarrow{\beta} = (\beta_1, \beta_2)$ are nonnegative. Let us consider a sub-grid that contains just one additional node P in each rectangular element. We will choose the point P, whose location may differ from element to element, along one of the diagonals of the rectangle K depending on the direction of the flow. The node P is then joined to the four vertices splitting the element K into four sub-triangles (see Fig. 1).

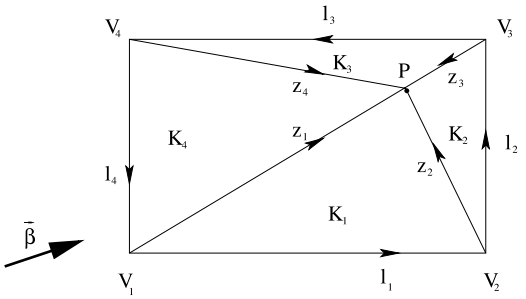

Fig. 1. Sub-grid configuration in a typical cell K.

Take an element K and a local numbering for its vertices $V_i = (x_i, y_i)$ $(i = 1, 2, 3, 4)$ using the counterclockwise order. Let us denote basis functions on K by b_p, φ_1, φ_2, φ_3 and φ_4. They are piecewise-linear functions on each sub-triangle K_i with the following property:

$$\begin{aligned} &b_P(P) = 1, \qquad b_P(V_i) = 0 \quad i = 1, 2, 3, 4 \\ &\varphi_i(V_i) = 1, \qquad \varphi_i(V_j) = 0 \quad j \neq i, \quad \text{and} \quad \varphi_i(P) = 0. \end{aligned} \tag{11}$$

Thus the basis function attached to the point P has support contained in K and the other four basis function have value one at one vertex and zero at P and at the other vertices. We further denote the edge of K adjacent to V_i by $\mathbf{l}_i$, the length of $\mathbf{l}_i$ by l_i, the outward unit normal to $\mathbf{l}_i$ by $\mathbf{n}_i$ and $\boldsymbol{\nu}_i = l_i \mathbf{n}_i$. The position of P along the diagonal from V_1 will be determined by the following condition: Choose P such that

$$a(\varphi_2, b_P)_K + 2a(\varphi_3, b_P)_K + a(\varphi_4, b_P)_K = 0. \tag{12}$$

Similar criteria were used in different configurations of the convection–diffusion problem [10,14]. The set of points on the diagonal connecting V_1 to V_3 can be described as a function depending on a single parameter t: $P = (1 - t)V_1 + tV_3$ where $0 < t < 1$. Then, denoting the area of K by $|K|$ and using the relations $\mathbf{m} = \mathbf{l}_1 + \mathbf{l}_2$ and $\mathbf{z}_1 = t\,\mathbf{m}$ together with

$$\nabla b_P = -l_i\,\mathbf{n}_i/2\,|K_i| \tag{13}$$

$$|K_1| = |K_4| = |K|\,t/2 \tag{14}$$

$$|K_2| = |K_3| = |K|\,(1 - t)/2 \tag{15}$$

we get

$$\begin{aligned} a(\varphi_2, b_P)_K &= \epsilon \left(-\frac{(\mathbf{z}_1, \mathbf{l}_1)}{4|K_1|} + \frac{(\mathbf{z}_3, \mathbf{l}_2)}{4|K_2|} \right) + \frac{1}{6}\,(\beta, \boldsymbol{\nu}_1 + \boldsymbol{\nu}_2) \\ a(\varphi_3, b_P)_K &= \epsilon \left(-\frac{(\mathbf{z}_2, \mathbf{l}_2)}{4|K_2|} + \frac{(\mathbf{z}_4, \mathbf{l}_1)}{4|K_3|} \right) + \frac{1}{6}\,(\beta, \boldsymbol{\nu}_2 + \boldsymbol{\nu}_3) \\ a(\varphi_4, b_P)_K &= \epsilon \left(+\frac{(\mathbf{z}_3, \mathbf{l}_1)}{4|K_3|} - \frac{(\mathbf{z}_1, \mathbf{l}_2)}{4|K_4|} \right) + \frac{1}{6}\,(\beta, \boldsymbol{\nu}_3 + \boldsymbol{\nu}_4). \end{aligned}$$

Adding the contributions coming from the diffusion terms and the convection terms separately, using the geometrical properties $\boldsymbol{\nu}_1 + \boldsymbol{\nu}_2 + \boldsymbol{\nu}_3 + \boldsymbol{\nu}_4 = 0$, $\mathbf{z}_2 - \mathbf{z}_3 = \mathbf{l}_2$, $\mathbf{z}_3 - \mathbf{z}_4 = \mathbf{l}_3 = -\mathbf{l}_1$, and then substituting the resulting expressions into the Eq. (12), we get

$$\epsilon \frac{h_K^2}{|K|\,(1 - t)} + \frac{1}{3}\,(\beta, \boldsymbol{\nu}_2 + \boldsymbol{\nu}_3) = 0. \tag{16}$$

Solving the Eq. (16) for t gives

$$t^* = 1 - \frac{3\,\epsilon\,h_K^2}{|K|\,(\beta, \boldsymbol{\nu}_2 + \boldsymbol{\nu}_3)}. \tag{17}$$

It is well known that if ϵ is not so small, the value provided by (17) could be meaningless [15]. Therefore the actual value of t that we take is

$$\begin{cases} t = t^* & \text{if } \epsilon \leq \epsilon^* = \dfrac{|K|(\beta, \boldsymbol{\nu}_2 + \boldsymbol{\nu}_3)}{6\,h_K^2} \\ t = 1/2 & \text{otherwise.} \end{cases} \tag{18}$$

Note that t continuously depends on ϵ and that $1/2 \leq t \leq 1$.

Remark 1. Another possible way of choosing the position of P was suggested in the context of pseudo-residual-free bubbles in [14] and further analyzed for triangular elements in [15]: Choose P such that the value of the integral

$$J(P) = \int_K |-\epsilon \triangle b_P^* + \beta \cdot \nabla b_P^* - 1| \mathrm{d}K \tag{19}$$

is minimum where $b_P^* = \alpha(P) b_P$ is the unique solution of

$$a(b_P^*, b_P)_K = (1, b_P) \quad \forall\, b_P. \tag{20}$$

We note that, although the bubble space B^K is spanned by two bubble basis functions for rectangular elements (see [8]), we consider the dominant one which is described by

$$\begin{cases} -\epsilon \triangle b_1 + \beta \cdot \nabla b_1 = 1 & \text{in } K \\ b_1 = 0 & \text{on } \partial K. \end{cases} \tag{21}$$

Indeed the criterion (19) aims to find an approximation b_P^* to the bubble basis function b_1. Following the lines of presentation in [15], the implementation of the criterion (19) exposes the value of t:

$$t^{**} = \begin{cases} 1 + \dfrac{3\,\epsilon\, h_K^2}{2|K|\,(\beta, \mathbf{v}_1)} = 1 - \dfrac{3\,\epsilon\, h_K^2}{2|K|\,(\beta, \mathbf{v}_3)} & \text{if } (\beta, \mathbf{v}_1) \le (\beta, \mathbf{v}_4) \\ 1 + \dfrac{3\,\epsilon\, h_K^2}{2|K|\,(\beta, \mathbf{v}_4)} = 1 - \dfrac{3\,\epsilon\, h_K^2}{2|K|\,(\beta, \mathbf{v}_2)} & \text{otherwise} \end{cases} \tag{22}$$

which qualitatively has the same structure with t^*. If $(\beta, \mathbf{v}_2) = (\beta, \mathbf{v}_3)$ both criteria (12) and (19) produce the same result for the location of P and the corresponding numerical methods are identical.

4. Error analysis

Let us return to the error analysis of the method (9) with the present choice of the sub-grid. In [13], Brezzi and Marini set abstract assumptions on a sub-grid in order to keep the same error performance for the corresponding method as we have for the SUPG method. We first give some definitions to be able to state these assumptions for the present configuration and then state the main result in a theorem. To this end, to every $v_h^A \in V_h^A$, let us associate two different elements, in a unique way, from V_h^A, that we call v_L and v_S by the conditions

$$v_L = v_S = v_h^A \quad \text{on} \bigcup_{K \in \tau_h} \partial K \quad \text{and} \quad v_L \in V_L, \quad v_S \in V_S \tag{23}$$

where ∂K represents the boundary of K and the subspaces V_L and V_S defined by

$$V_L = \{v_L \in V_h^A \text{ such that: } a(v_L, v_B) = 0\ \forall\, v_B \in B_h^K\} \tag{24}$$

$$V_S = \{v_S \in V_h^A \text{ such that: } (\nabla v_S, \nabla v_B) = 0\ \forall\, v_B \in B_h^K\}. \tag{25}$$

Theorem 1. *Assume that the sub-grid is made of a single internal node P in each element and let the sub-grid node P be chosen according to (18). Assume further that the bubble space satisfies the following two assumptions;*

$$\exists C_2 : \forall K \in \tau_h, \quad \|b_P\|_{0,K} \le C_2\, h_K^{1/2}\, \epsilon^{1/2}\, |b_P|_{1,K} \tag{26}$$

and

$$\exists C_3 : \forall K \in \tau_h,\ \forall v_h^A \in V_h^A, \quad \|\beta \cdot \nabla v_S\|_{0,K} \le C_3\, h_K^{-1/2}\, \epsilon^{1/2} \|\nabla v_L\|_{0,K}. \tag{27}$$

Let u and u_h be the solutions of (2) and (9) respectively, and assume that $u \in H^s(\Omega)$ for some s with $1 < s \le 2$. Then there exist a constant C, independent of h, such that

$$\epsilon |u - u_h|_{1,\Omega}^2 + \sum_{K \in \tau_h} h_K \|\beta \cdot \nabla (u - u_h)\|_{0,K}^2 \le C \sum_{K \in \tau_h} \left(\epsilon h_K^{2s-2} + h_K^{2s-1}\right) |u|_{s,K}^2. \tag{28}$$

We will prove that the conditions (26) and (27) in Theorem 1 are satisfied for the present choice of P. Thus we will conclude that standard Galerkin finite element method on the augmented grid produces a discrete solution that satisfies a priori error estimate (28) by means of Theorem 1.

Lemma 1. *Assume that, for every element $K \in \tau_h$, the position of the internal node P is chosen according to (18). Then*

$$|b_p|_1^2 = \begin{cases} \dfrac{A^2\,|K|}{2\,\epsilon\,(A\,|K| - \epsilon\, h^2)} \sim O\left(\dfrac{h}{\epsilon}\right) & \text{if } \epsilon \le \epsilon^* \\ 2\,h_K^2/|K| \sim O(1) & \text{otherwise} \end{cases}$$

where

$$A = \frac{\boldsymbol{\beta}}{3} \cdot (l_2 \mathbf{n}_2 + l_3 \mathbf{n}_3).$$

Proof. We use the relations (13)–(15) to obtain

$$|b_P|_1^2 = \int_K |\nabla b_P|^2 = \sum_{i=1}^{4} \int_{K_i} |\nabla b_P|^2 = \frac{l_1^2 + l_2^2}{4} \left(\frac{1}{|K_1|} + \frac{1}{|K_2|} \right) = \frac{l_1^2 + l_2^2}{2\,|K|} \left(\frac{1}{t} + \frac{1}{1-t} \right).$$

Lemma follows by substituting the value of t in (18) into the last expression. □

Now using Lemma 1, we can prove that the first condition (26) is satisfied for the present choice of P.

Proposition 1. *Assume that, for every element $K \in \tau_h$, the position of the internal node P is chosen according to (18). Then the condition (26) is satisfied.*

Proof. We need to prove that the supremum

$$\sup_{\epsilon > 0} \frac{\|b_P\|_{0,K}}{h^{1/2}\,\epsilon^{1/2}\,|b_P|_{1,K}} \tag{29}$$

is uniformly bounded with respect to element diameter h. Consider the case $\epsilon < \epsilon^*$ first. Since b_p is linear over in each sub-triangle K_i, we can use the integration formula that uses the midpoints of the edges for computing the integral of its square and get

$$\int_K b_p^2 = \frac{|K|}{6}. \tag{30}$$

On the other hand, the shape regularity condition (10) implies that

$$A = \frac{\boldsymbol{\beta}}{3} \cdot (l_2 \mathbf{n}_2 + l_3 \mathbf{n}_3) \geq \frac{\boldsymbol{\beta}}{3} \cdot (\mathbf{n}_2 + \mathbf{n}_3) \min\{l_1, l_2\} \geq \frac{\boldsymbol{\beta}}{3} \cdot (\mathbf{n}_2 + \mathbf{n}_3)\, C_1 h \tag{31}$$

and the inequality $ab \leq (a^2 + b^2)/2$ leads to

$$|K| \leq \frac{h^2}{2}. \tag{32}$$

Using (29) together with (30), (31) and (32), respectively, we get

$$\frac{\|b_P\|_{0,K}^2}{h\,\epsilon\,|b_P|_{1,K}^2} = \frac{|K|}{3\,A\,h} - \frac{\epsilon\,h}{3\,A^2} \leq \frac{|K|}{3\,A\,h} \leq \frac{|K|}{\boldsymbol{\beta} \cdot (\mathbf{n}_2 + \mathbf{n}_3)\, C_1 h^2} \leq \frac{1}{2\,\boldsymbol{\beta} \cdot (\mathbf{n}_2 + \mathbf{n}_3)\, C_1}$$

which is independent of h and ϵ. Secondly, when $\epsilon \geq \epsilon^*$, use (29), $\epsilon^* = \frac{|K|(\boldsymbol{\beta}, \mathbf{v}_2 + \mathbf{v}_3)}{6\,h^2}$ and (30)–(32), respectively, to get

$$\begin{aligned} \frac{\|b_P\|_{0,K}^2}{h\,\epsilon\,|b_P|_{1,K}^2} &\leq \frac{|K|^2}{12\,\epsilon\,h^3} \leq \frac{|K|^2}{12\,\epsilon^*\,h^3} \leq \frac{|K|}{2\,\boldsymbol{\beta} \cdot (\mathbf{v}_2 + \mathbf{v}_3)\,h} \\ &\leq \frac{|K|}{2\,\boldsymbol{\beta} \cdot (\mathbf{n}_2 + \mathbf{n}_3)\, C_1\, h^2} \leq \frac{1}{4\,\boldsymbol{\beta} \cdot (\mathbf{n}_2 + \mathbf{n}_3)\, C_1} \end{aligned}$$

which is again independent of h and ϵ and the result follows. □

To prove that the second condition (27) holds true with the present choice of the sub-grid, we need the following preliminary results.

Lemma 2. *For an arbitrary $v_h^A \in V_h^A$, let v_L and v_S be defined as in (24) and (25), respectively. Then*

$$\|\nabla v_L\|_0^2 = \|\nabla v_S\|_0^2 + \frac{1}{\epsilon^2\,\|\nabla b_P\|_0^2} \left(\int_K \beta \cdot \nabla v_S\, b_P \,\mathrm{d}K \right)^2.$$

Proof. From (23), we have $v_L = v_S + \mu\, b_P$, where μ is a scalar to be determined. Now

$$\begin{aligned} a(v_L, b_P)_K &= a(v_S + \mu b_P, b_P)_K \\ &= \epsilon(\nabla v_S, \nabla b_P) + (\beta \cdot \nabla v_S, b_P) + \epsilon(\mu \nabla b_P, \nabla b_P) + \mu(\beta \cdot \nabla b_P, b_P) \\ &= (\beta \cdot \nabla v_S, b_P) + \epsilon(\mu \nabla b_P, \nabla b_P) \end{aligned}$$

since the expressions $\epsilon(\nabla v_S, \nabla b_P)$ and $\mu(\beta \cdot \nabla b_P, b_P)$ vanish by definition (25) and the integration by parts, respectively. From the resulting expression and the relation $a(v_L, b_P)_K = 0$, we can deduce the unique value of μ:

$$\mu = -\frac{(\beta \cdot \nabla v_S, b_P)}{\epsilon \|\nabla b_P\|_0^2}$$

with which, the function v_L becomes

$$v_L = v_S - \frac{(\beta \cdot \nabla v_S, b_P)}{\epsilon \|\nabla b_P\|_0^2} b_P. \tag{33}$$

The result follows from (33) and using the orthogonality of v_S and b_P with respect to the product $(\nabla\cdot, \nabla\cdot)$:

$$\begin{aligned}
\|\nabla v_L\|_0^2 &= (\nabla v_L, \nabla v_L) \\
&= \left(\nabla v_S - \frac{(\beta \cdot \nabla v_S, b_P)}{\epsilon \|\nabla b_P\|_0^2} \nabla b_P \,,\; \nabla v_S - \frac{(\beta \cdot \nabla v_S, b_P)}{\epsilon \|\nabla b_P\|_0^2} \nabla b_P\right) \\
&= (\nabla v_S, \nabla v_S) - 2\,\frac{(\beta \cdot \nabla v_S, b_P)}{\epsilon \|\nabla b_P\|_0^2} (\nabla v_S, \nabla b_P) + \frac{(\beta \cdot \nabla v_S, b_P)^2}{\epsilon^2 \|\nabla b_P\|_0^4} (\nabla b_P, \nabla b_P) \\
&= \|\nabla v_S\|_0^2 + \frac{(\beta \cdot \nabla v_S, b_P)^2}{\epsilon^2 \|\nabla b_P\|_0^2}. \quad \square
\end{aligned}$$

Now we want to replace the function v_S with its a smoother counterpart φ for the sake of computational simplicity. In that context, given the function v_S, we define a new function φ to be the solution of the following Dirichlet problem

$$\begin{cases} \triangle\varphi = 0 & \text{in K}, \\ \varphi = v_S & \text{on } \partial K. \end{cases} \tag{34}$$

So the function v_S is the standard finite element approximation to the function φ which is a bilinear function over K and they satisfy $\|\nabla(\varphi - v_S)\| \le C\,h$; C being a generic constant. We note that v_S and φ are close enough to each other to make an interchange between them. Hence we will deal with the term $(\beta \cdot \nabla\varphi, b_P)$ instead of $(\beta \cdot \nabla v_S, b_P)$. Having this replacement done, we can easily reveal the dependence of the integral $\int_K \beta \cdot \nabla\varphi\, b_P\, \mathrm{d}K$ to the sub-grid node P in an explicit manner:

Lemma 3. *Let φ be an arbitrary bilinear function on K. Then we have*

$$\int_K \beta \cdot \nabla\varphi\, b_P\, \mathrm{d}K = \int_K \left(\frac{1}{3}\beta \cdot \nabla\varphi(\mathbf{x}_K) + \frac{1}{12}\,\beta^T \cdot (\mathbf{x}_P - \mathbf{x}_K)\,\varphi_{xy}\right) \mathrm{d}K \tag{35}$$

where $\beta^T = (\beta_2, \beta_1)$.

Proof. Let $\mathbf{x}_K$ be the barycenter of K. Since φ is a bilinear function on K, the representation

$$\beta \cdot \nabla\varphi = \beta \cdot \nabla\varphi(\mathbf{x}_K) + \beta^T \cdot (\mathbf{x} - \mathbf{x}_K)\,\varphi_{xy} \tag{36}$$

holds true. Multiplying both sides of (36) by b_P and integrating over K, we have

$$\begin{aligned}
\int_K \beta \cdot \nabla\varphi\, b_P\, \mathrm{d}K &= \beta \cdot \nabla\varphi(\mathbf{x}_K) \int_K b_P\, \mathrm{d}K + \varphi_{xy}|_K \int_K \beta^T \cdot (\mathbf{x} - \mathbf{x}_K)\, b_P\, \mathrm{d}K \\
&= \beta \cdot \nabla\varphi(\mathbf{x}_K)\,\frac{|K|}{3} + \varphi_{xy}|_K \int_K \beta^T \cdot (\mathbf{x} - \mathbf{x}_K)\, b_P\, \mathrm{d}K \\
&= \frac{1}{3}\int_K \beta \cdot \nabla\varphi(\mathbf{x}_K)\, \mathrm{d}K + \varphi_{xy}|_K \int_K \beta^T \cdot (\mathbf{x} - \mathbf{x}_K)\, b_P\, \mathrm{d}K.
\end{aligned} \tag{37}$$

Next we calculate the second integral on the right-hand side of (37). Since b_P is linear in each sub-triangle K_i, $\beta^T \cdot (\mathbf{x} - \mathbf{x}_K)\, b_P$ is a quadratic function on K_i whose integral can be computed exactly by using the midpoint rule: Define

$$\begin{aligned}
x_{ij} &= \frac{x_i + x_j}{2} \qquad x_{iP} = \frac{x_i + x_P}{2} \quad i, j = 1, 2, 3, 4 \\
y_{ij} &= \frac{y_i + y_j}{2} \qquad y_{iP} = \frac{y_i + y_P}{2} \quad i, j = 1, 2, 3, 4
\end{aligned}$$

and use the geometrical properties

$$\begin{aligned}
&x_{12} - x_K = x_{34} - x_K = 0 \\
&y_{23} - y_K = y_{41} - y_K = 0 \\
&x_{23} - x_K = x_K - x_{41} = l_1/2 \\
&y_{34} - y_K = y_K - y_{12} = l_2/2 \\
&|K_1| - |K_3| = l_1(y_P - y_K) \\
&|K_4| - |K_2| = l_2(x_P - x_K)
\end{aligned}$$

to evaluate the second integral on the right-hand side of (37):

$$
\begin{aligned}
\int_K \beta^T\cdot(\mathbf{x}-\mathbf{x}_K)\,b_P\,\mathrm{d}K &= \sum_{i=1}^{4}\int_{K_i}\beta^T\cdot(\mathbf{x}-\mathbf{x}_K)\,b_P\,\mathrm{d}K\\
&= \frac{|K_1|}{3}\left[\beta^T\cdot(x_{1P}-x_K,y_{1P}-y_K)\frac{1}{2}+\beta^T\cdot(x_{2P}-x_K,y_{2P}-y_K)\frac{1}{2}\right]\\
&\quad+\frac{|K_2|}{3}\left[\beta^T\cdot(x_{2P}-x_K,y_{2P}-y_K)\frac{1}{2}+\beta^T\cdot(x_{3P}-x_K,y_{3P}-y_K)\frac{1}{2}\right]\\
&\quad+\frac{|K_3|}{3}\left[\beta^T\cdot(x_{3P}-x_K,y_{3P}-y_K)\frac{1}{2}+\beta^T\cdot(x_{4P}-x_K,y_{4P}-y_K)\frac{1}{2}\right]\\
&\quad+\frac{|K_4|}{3}\left[\beta^T\cdot(x_{4P}-x_K,y_{4P}-y_K)\frac{1}{2}+\beta^T\cdot(x_{1P}-x_K,y_{1P}-y_K)\frac{1}{2}\right]\\
&= \frac{|K_1|}{6}[\beta_2(x_{1P}+x_{2P}-2x_K)+\beta_1(y_{1P}+y_{2P}-2y_K)]+\frac{|K_2|}{6}[\beta_2(x_{2P}+x_{3P}-2x_K)+\beta_1(y_{2P}+y_{3P}-2y_K)]\\
&\quad+\frac{|K_3|}{6}[\beta_2(x_{3P}+x_{4P}-2x_K)+\beta_1(y_{3P}+y_{4P}-2y_K)]+\frac{|K_4|}{6}[\beta_2(x_{4P}+x_{1P}-2x_K)+\beta_1(y_{4P}+y_{1P}-2y_K)]\\
&= \frac{|K_1|}{6}[\beta_2(x_{12}+x_P-2x_K)+\beta_1(y_{12}+y_P-2y_K)]+\frac{|K_2|}{6}[\beta_2(x_{23}+x_P-2x_K)+\beta_1(y_{23}+y_P-2y_K)]\\
&\quad+\frac{|K_3|}{6}[\beta_2(x_{34}+x_P-2x_K)+\beta_1(y_{34}+y_P-2y_K)]+\frac{|K_4|}{6}[\beta_2(x_{41}+x_P-2x_K)+\beta_1(y_{41}+y_P-2y_K)]\\
&= \frac{|K_1|}{6}\left[\beta_2(x_P-x_K)+\beta_1\left(-\frac{l_2}{2}+y_P-y_K\right)\right]+\frac{|K_2|}{6}\left[\beta_2\left(\frac{l_1}{2}+x_P-x_K\right)+\beta_1(y_P-y_K)\right]\\
&\quad+\frac{|K_3|}{6}\left[\beta_2(x_P-x_K)+\beta_1\left(\frac{l_2}{2}+y_P-y_K\right)\right]+\frac{|K_4|}{6}\left[\beta_2\left(-\frac{l_1}{2}+x_P-x_K\right)+\beta_1(y_P-y_K)\right]\\
&= \frac{|K|}{6}\beta^T\cdot(\mathbf{x}_P-\mathbf{x}_K)+\frac{|K_1|}{6}\beta_1\left(-\frac{l_2}{2}\right)+\frac{|K_2|}{6}\beta_2\left(\frac{l_1}{2}\right)+\frac{|K_3|}{6}\beta_1\left(\frac{l_2}{2}\right)+\frac{|K_4|}{6}\beta_2\left(-\frac{l_1}{2}\right)\\
&= \frac{|K|}{6}\beta^T\cdot(\mathbf{x}_P-\mathbf{x}_K)-\frac{\beta_1 l_2 l_1}{12}(y_P-y_K)-\frac{\beta_2 l_1 l_2}{12}(x_P-x_K)\\
&= \frac{|K|}{6}\beta^T\cdot(\mathbf{x}_P-\mathbf{x}_K)-\frac{|K|}{12}\beta^T\cdot(\mathbf{x}_P-\mathbf{x}_K)\\
&= \frac{|K|}{12}\beta^T\cdot(\mathbf{x}_P-\mathbf{x}_K).
\end{aligned}
$$

Thus, starting from (37), we get

$$
\begin{aligned}
\int_K \beta\cdot\nabla\varphi\,b_P\,\mathrm{d}K &= \frac{1}{3}\int_K\beta\cdot\nabla\varphi(\mathbf{x}_K)\,\mathrm{d}K+\varphi_{xy}|_K\int_K\beta^T\cdot(\mathbf{x}-\mathbf{x}_K)\,b_P\,\mathrm{d}K\\
&= \frac{1}{3}\int_K\beta\cdot\nabla\varphi(\mathbf{x}_K)\,\mathrm{d}K+\varphi_{xy}|_K\frac{|K|}{12}\beta^T\cdot(\mathbf{x}_P-\mathbf{x}_K)\\
&= \frac{1}{3}\int_K\beta\cdot\nabla\varphi(\mathbf{x}_K)\,\mathrm{d}K+\frac{1}{12}\int_K\beta^T\cdot(\mathbf{x}_P-\mathbf{x}_K)\,\varphi_{xy}\,\mathrm{d}K
\end{aligned}
$$

which is the desired result. □

Now we are ready to prove that the second condition (27) holds with the present choice of P.

Proposition 2. *Assume that, for every $K\in\tau_h$, the position of the internal node is chosen according to (18). Then the condition (27) holds true.*

Proof. We need to prove that the supremum

$$
\sup_{\epsilon>0}\frac{h\,\|\beta\cdot\nabla\varphi\|_{0,K}^2}{\epsilon\,\|\nabla v_L\|_{0,K}^2} \tag{38}
$$

is uniformly bounded with respect to element diameter h. The expression (38) can be rewritten more precisely by using Lemma 2;

$$\sup_{\epsilon>0} \frac{h \|\beta \cdot \nabla\varphi\|^2_{0,K}}{\epsilon \|\nabla\varphi\|^2_0 + \frac{1}{\epsilon \|\nabla b_P\|^2_0} (\int_K \beta \cdot \nabla\varphi \, b_P \, \mathrm{d}K)^2} \tag{39}$$

and we will prove that it exists when $\epsilon < \epsilon^*$. The case when $\epsilon > \epsilon^*$ is similar but easier. Now, by using the decomposition (36), let us observe that a direct calculation of the double integral over the region K gives

$$\begin{aligned} \|\beta \cdot \nabla\varphi\|^2_0 &= \int_K \left(\beta \cdot \nabla\varphi(\mathbf{x}_K) + \beta^T \cdot (\mathbf{x} - \mathbf{x}_K)\, \varphi_{xy}\right)^2 \mathrm{d}K \\ &= \int_K (\beta \cdot \nabla\varphi(\mathbf{x}_K))^2 \, \mathrm{d}K + \int_K \frac{\beta_2^2 l_1^2 + \beta_1^2 l_2^2}{12} \varphi_{xy}^2 \, \mathrm{d}K. \end{aligned} \tag{40}$$

On the other hand, from Lemma 3, we have

$$\int_K \beta \cdot \nabla\varphi \, b_P \, \mathrm{d}K = \int_K \left(\frac{1}{3}\beta \cdot \nabla\varphi(\mathbf{x}_K) + \frac{1}{12} \beta^T \cdot (\mathbf{x}_P - \mathbf{x}_K)\, \varphi_{xy}\right) \mathrm{d}K. \tag{41}$$

Since $0 \le |\mathbf{x}_P - \mathbf{x}_K| \le h/2$, the last term in (41) is of order h. That implies if $\int_K \beta \cdot \nabla\varphi \, b_P \, \mathrm{d}K = 0$ then $\beta \cdot \nabla\varphi = 0$ in the interesting case where a layer structure exist and, thus, the assumption (27) is satisfied. Now suppose that $\int_K \beta \cdot \nabla\varphi \, b_P \, \mathrm{d}K \neq 0$. Again, since the last terms in (40) and (41) are of order h^2 and h, respectively, we may assume that there exist a positive constant C_4, independent of h and ϵ, such that

$$C_4 \, h^2 \, \|\beta \cdot \nabla\varphi\|^2_0 \le \left(\int_K \beta \cdot \nabla\varphi \, b_P \, \mathrm{d}K\right)^2 \tag{42}$$

holds true in the interesting case where a layer structure exist. Now recall that, Lemma 1 ensures that there exist a constant C_5, depending only on β and the shape regularity condition of K, such that

$$\|\nabla b_P\|^2_0 \le C_5 \, \frac{h}{\epsilon} \tag{43}$$

is satisfied. Finally, using (42), the fact that $\|\beta \cdot \nabla\varphi\| \le 2\,\beta_{max} \, \|\nabla\varphi\|$, with $\beta_{max} = \max\{|\beta_1|, |\beta_2|\}$, and the inequality (43), respectively, we get

$$\begin{aligned} \frac{h \|\beta \cdot \nabla\varphi\|^2_{0,K}}{\epsilon \|\nabla v_L\|^2_{0,K}} &\le \frac{h \|\beta \cdot \nabla\varphi\|^2_{0,K}}{\epsilon \|\nabla\varphi\|^2_0 + \frac{C_4 h^2 \|\beta \cdot \nabla\varphi\|^2_0}{\epsilon \|\nabla b_P\|^2_0}} \\ &\le \frac{h \|\beta \cdot \nabla\varphi\|^2_{0,K}}{\frac{\epsilon \|\beta \cdot \nabla\varphi\|^2_0}{4\,\beta^2_{max}} + \frac{C_4 h^2 \|\beta \cdot \nabla\varphi\|^2_0}{\epsilon \|\nabla b_P\|^2_0}} \\ &\le \frac{h}{\frac{\epsilon}{4\,\beta^2_{max}} + \frac{C_4 h^2}{\epsilon \|\nabla b_P\|^2_0}} \\ &\le \frac{h}{\frac{\epsilon}{4\,\beta^2_{max}} + \frac{C_4 h^2}{\epsilon\, C_5\, h/\epsilon}} \\ &\le \frac{4\,\beta^2_{max}\, C_5\, h}{\epsilon\, C_5 + 4\,\beta^2_{max}\, C_4\, h} \le \frac{C_5}{C_4} \end{aligned}$$

and the result follows. □

5. Numerical results

In this section, we will present some numerical results showing the stabilizing features of the method under consideration. We remark that the sub-grid node is chosen according to the criteria (12). We will solve the problem (1)

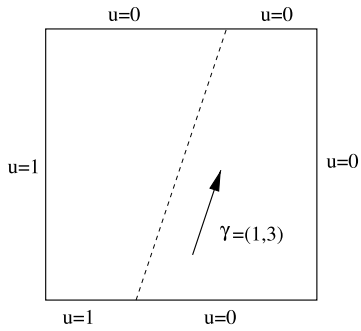

Fig. 2. Configuration of the test problem.

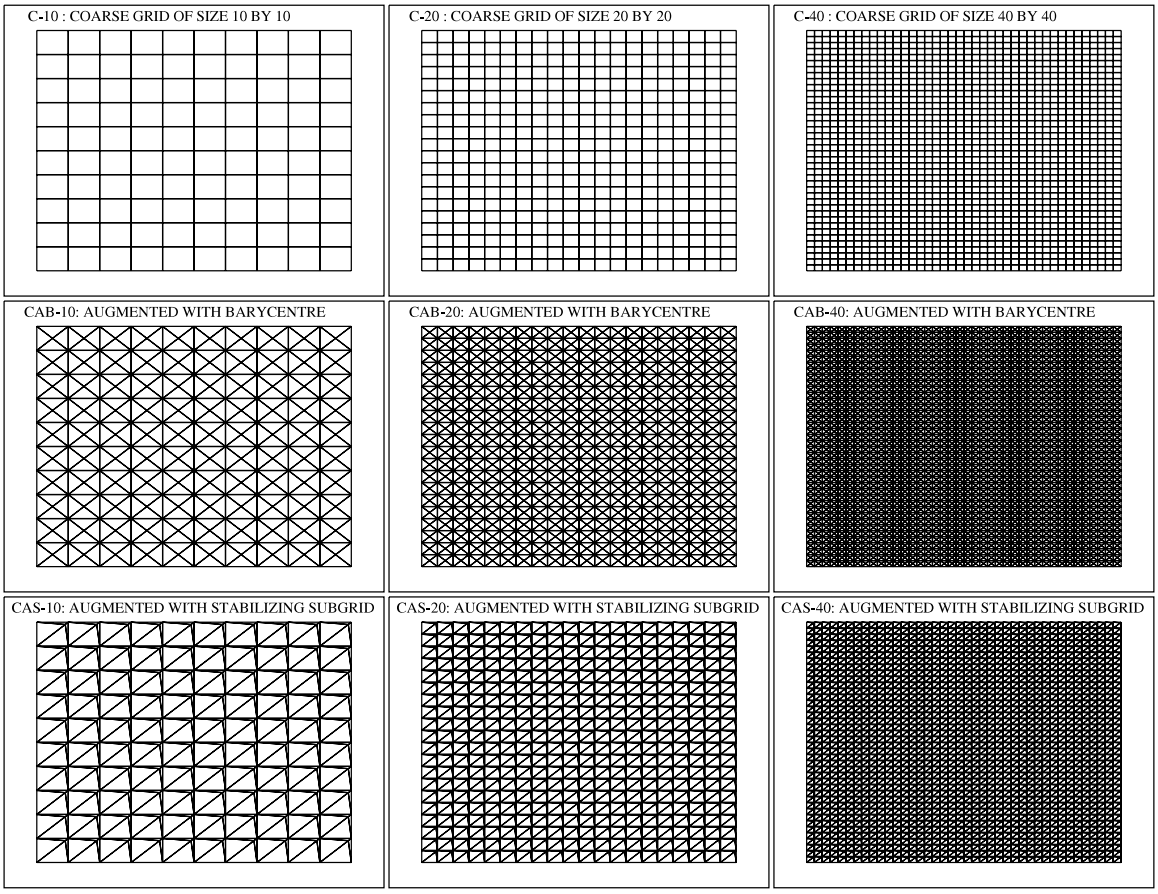

Fig. 3. Coarse meshes (1st row) and the corresponding augmented meshes (2nd and 3rd rows).

with $f = 0$ and a nonzero Dirichlet boundary condition on a computational domain $\Omega = [0, 1] \times [0, 1]$ described in Fig. 2. We take a midrange value for ϵ; $\epsilon = 0.001$. $\beta = \gamma/|\gamma|$.

We first present the standard Galerkin solution of the problem on a set of successively refined meshes and compare the solutions on two classes of augmented meshes. We start by taking a set of coarse meshes which are made of 100, 400 and 1600 uniform rectangular elements. We augment each coarse mesh by adding a single internal node into each element and then joining the additional point to the grid points of the coarse mesh, thus forming four sub-triangles in each element of coarse mesh. In the first choice, displayed in the second row in Fig. 3, we take the sub-grid node to be the barycentric coordinate of the cell K without taking the value of ϵ into consideration. In the second choice, we locate the sub-grid node according to (18) and it is displayed in the last row in Fig. 3.

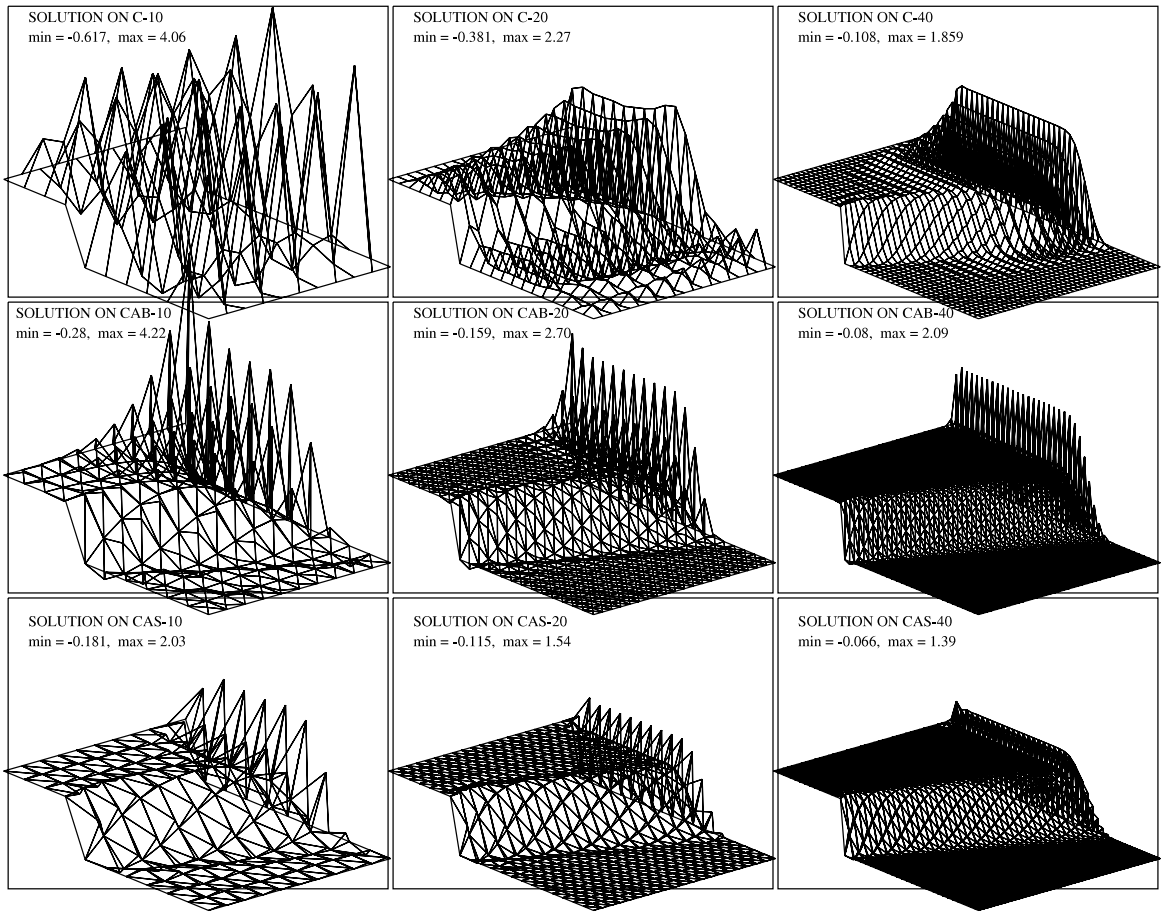

Fig. 4. Elevation plots of the solutions.

The elevation plots of the standard Galerkin solution on three types of meshes are shown in Fig. 4. Numerical solutions were obtained by using standard bilinear shape functions over the coarse meshes and standard linear shape functions over the augmented meshes of triangles. The test problem has an exact solution that exhibits an internal and a boundary layer. It is clear that the numerical solution obtained by the algorithm introduced herein is able to show the dominant characteristics of the exact solution at all levels of the mesh employed. Comparing two types of augmented meshes, we can conclude that the stabilizing effect of the method fairly depends on the enrichment of the grid by means of a suitably chosen sub-grid. Finally, we note that the numerical solution obtained over the mesh augmented with the stabilizing sub-grid is comparable with the approximation obtained over the next level refinement of the uniform mesh in the first row (compare solutions obtained over the meshes C-40 and CAS-20, for example).

Secondly, we want to inspect the numerical method over the mesh augmented with the stabilizing sub-grid when the streamlines are aligned with the diagonals of the elements, in which case the stabilizing term in the RFB method is not equivalent to the mesh-dependent stabilizing term in the SUPG method. The elevation plots of the standard Galerkin solution over the fine meshes augmented with the stabilizing sub-grids are shown in Fig. 5. We can conclude that the numerical solutions in this exceptional case are still good enough and retain the characteristic features of the exact solution quite well.

6. Conclusion

A rectangular mesh augmented with a properly chosen sub-grid is proposed and analyzed for solving the convection–diffusion problem in the framework of the standard Galerkin finite element method. The choice of the additional sub-grid node in a typical rectangular element is described. We proved that the discrete solution on augmented grid with the present choice of the sub-grid satisfies the same a priori error estimates that are typically obtained with the SUPG method. Numerical experiments presented confirm the theoretical findings.

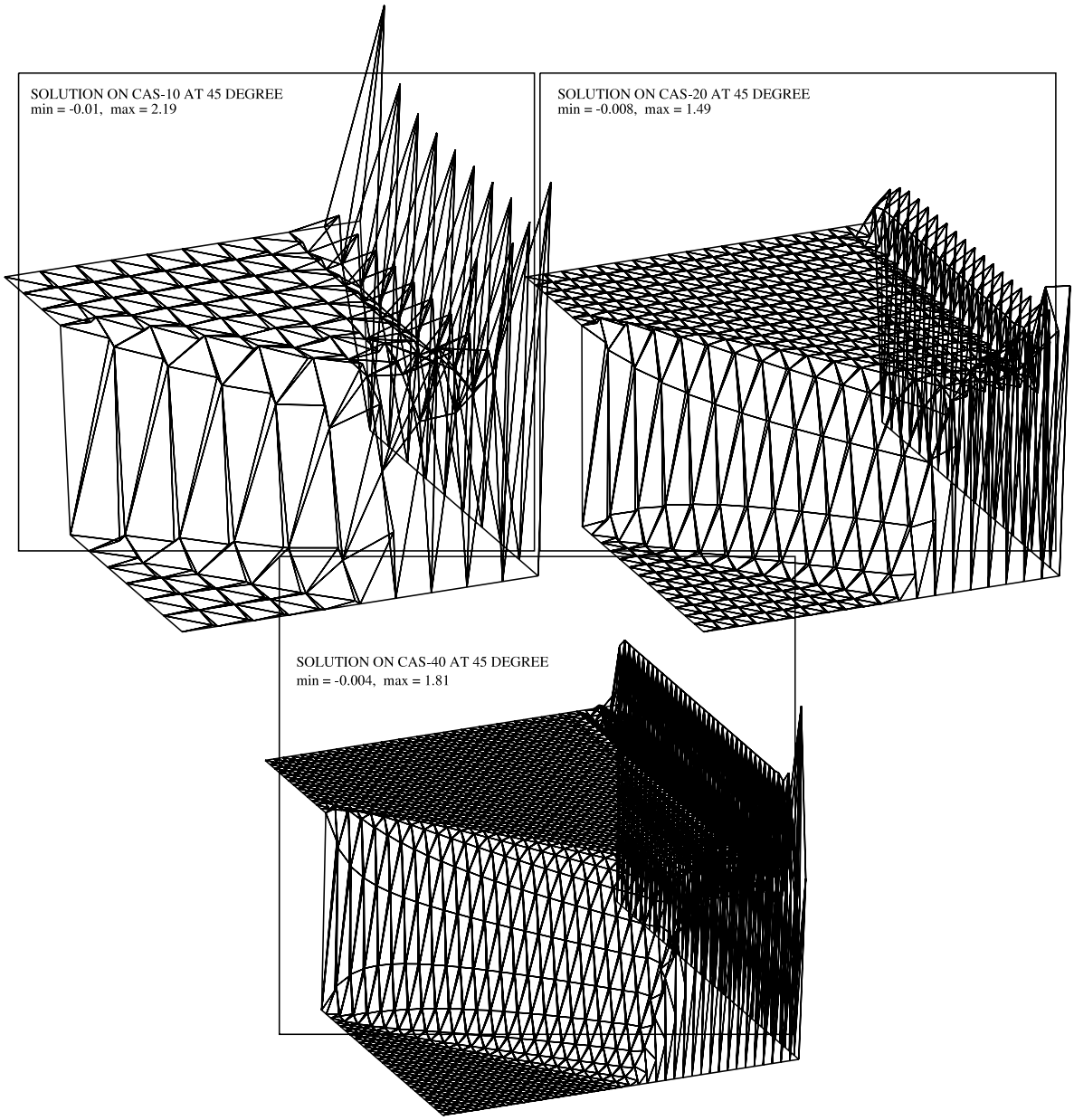

Fig. 5. Elevation plots of the solutions when the flow is aligned with the diagonal of the element.

References

[1] F. Brezzi, A. Russo, Choosing bubbles for advection–diffusion problems, Math. Models Methods Appl. Sci. 4 (1994) 571–587.
[2] L.P. Franca, S.L. Frey, T.J.R. Hughes, Stabilized finite element methods: I. Application to the advective–diffusive model, Comput. Methods Appl. Mech. Engrg. 95 (1992) 253–276.
[3] L.P. Franca, A. Nesliturk, M. Stynes, On the stability of residual-free bubbles for convection–diffusion problems and their approximation by a two-level finite element method, Comput. Methods Appl. Mech. Engrg. 166 (1998) 35–49.
[4] F. Brezzi, T.J.R. Hughes, L.D. Marini, A. Russo, E. Suli, A priori error analysis of Residual-free bubbles for advection–diffusion problems, SIAM J. Numer. Anal. 36 (1999) 1933–1948.
[5] U. Risch, Convergence analysis of the Residual free bubble method for bilinear elements, SIAM J. Numer. Anal. 39 (2001) 1366–1379.
[6] G. Sangalli, Global and local error analysis for the residual-free bubbles method applied to advection-dominated problems, SIAM J. Numer. Anal. 38 (2000) 1496–1522.
[7] F. Brezzi, M.O. Bristeau, L.P. Franca, M. Mallet, G. Rogé, A relationship between stabilized finite element methods and the Galerkin method with bubble functions, Comput. Methods Appl. Mech. Engrg. 96 (1992) 117–129.
[8] L.P. Franca, L. Tobiska, Stability of the residual free bubble method for bilinear finite elements on rectangular grids, IMA J. Numer. Anal. 22 (2002) 73–87.
[9] F. Brezzi, D. Marini, A. Russo, Applications of the pseudo residual-free bubbles to the stabilization of convection–diffusion problems, Comput. Methods Appl. Mech. Engrg. 166 (1998) 51–63.

[10] F. Brezzi, G. Hauke, D. Marini, G. Sangalli, Link-cutting bubbles for the stabilization of convection–diffusion–reaction problems, Math. Models Methods Appl. Sci. 13 (2003) 445–461.
[11] L.P. Franca, A. Nesliturk, On a two-level finite element method for the incompressible Navier–Stokes equations, Inter. J. Numer. Methods Engrg. 52 (2001) 433–453.
[12] A. Masud, R.A. Khurram, A multiscale/stabilized finite element method for the advection–diffusion equation, Comput. Methods Appl. Mech. Engrg. 193 (2004) 1997–2018.
[13] F. Brezzi, D. Marini, Augmented spaces, two-level methods, and stabilizing sub-grids, Inter. J. Numer. Methods Fluids 40 (2002) 31–46.
[14] F. Brezzi, D. Marini, A. Russo, On the choice of a stabilizing subgrid for convection–diffusion problems, Comput. Methods Appl. Mech. Engrg. 194 (2005) 127–148.
[15] A. Nesliturk, A stabilizing subgrid for convection–diffusion problem, Math. Models Methods Appl. Sci. 16 (2006) 211–232.